g factors of $\frac{9}{2}^-$ and $\frac{23}{2}^+$ isomeric states in ^{129}Ba

Jasmeet Kaur,[1] A. K. Bhati,[1,*] N. Bansal,[1] V. Kumar,[2] Vijay R. Sharma,[3] H. Kumar,[3] R. Kumar,[4] and R. K. Bhowmik[4]

[1]*Centre for Advanced Studies in Physics, Panjab University, Chandigarh 160 014, India*

[2]*Centre for Medical Physics, Panjab University, Chandigarh 160 014, India*

[3]*Department of Physics, A.M. University, Aligarh 202 002, India*

[4]*Inter-University Accelerator Centre, JNU Campus, New Delhi 110 067, India*

(Received 18 February 2013; published 21 June 2013)

The time differential perturbed angular distribution (TDPAD) technique has been used to measure the g factor of the 173 keV $\frac{9}{2}^-$ and 2162 keV $\frac{23}{2}^+$ isomeric states in ^{129}Ba with respect to the known value of the g factor, $-0.159(5)$, of the 10^+ isomeric state in ^{132}Ba. The measured internal magnetic field at ^{132}Ba in Fe at room temperature is $-6.0(2)$ T. The extracted $g(\frac{9}{2}^-)$ value, $-0.192(6)$, is consistent with the pure $\nu\frac{9}{2}^-[514]$ Nilsson configuration while the $g(\frac{23}{2}^+)$ value, $-0.233(7)$, corresponds to the proposed three-quasineutron configuration $\frac{5}{2}^+[402]\otimes\frac{7}{2}^-[523]\otimes\frac{11}{2}^-[505]$ with the admixture of $\nu\frac{7}{2}^+[404]\otimes\frac{7}{2}^-[523]\otimes\frac{9}{2}^-[514]$ configuration.

DOI: 10.1103/PhysRevC.87.064312 PACS number(s): 21.10.Ky, 21.60.Ev, 27.60.+j, 76.60.Jx

I. INTRODUCTION

The neutron-deficient barium nuclei belong to the transitional region, $N = 66$ to $N = 82$, characterized by γ softness, triaxiality and the occupancy of the unique parity $h_{11/2}$ shell by the protons and the neutrons. The variety of shapes is expected because of the opposite shape driving properties of protons and neutrons occupying low-Ω and high-Ω orbitals, respectively [1]. There is similarity in the excitation and the pair breaking energy of the protons and neutrons which results in the strong competition between proton and neutron excitations within the shell, as in the case of S bands in some of the even-even Xe and Ba nuclei [2]. The transitional region is ideal ground to investigate the interplay between the single-particle and the collective degrees of freedom and the associated polarization of the core. The rotation and the quasiparticle alignment contribute additional structural effects. In addition, the occupancy of high-Ω orbitals has resulted in the formation of K isomers. The K quantum number (defined as the sum of the projection of angular momenta of the constituent quasiparticles on the symmetry axis) analogous to the $A \sim 170$–180 mass region may not be a good quantum number because of the effective triaxiality [3]. A variety of mechanisms [4] have been proposed and it is crucial to know the nature of the participating nucleons in the formation of the state. In-beam γ-ray spectroscopy together with neutron pickup and nuclear moment measurements have been used for the elucidation of the complicated level scheme. Unfortunately, very few nuclear moment measurements have been performed for the excited states in this mass region. The low-lying states are interpreted within the framework of the rigid-triaxial-rotor model (RTRM) [5] or alternatively using the algebraic model [6,7].

Fast laser beam spectroscopy has provided systematic data of the nuclear electromagnetic moments of the ground state in the Xe-Ba-Ce mass region, and its interpretation based on the triaxial-core plus particle formalism has confirmed the triaxiality ($\gamma \approx 20^\circ$–30°) in the ground state with moderate deformation ($\beta \approx 0.14$–0.26) [8]. The ^{129}Ba nucleus falls in the transitional region and the low-energy level structure is explained qualitatively based on the coupling of odd neutrons to the softest even-even ^{128}Ba triaxial core [9] in this region.

Three isomeric states, 8 keV $K^\pi = \frac{7}{2}^+$, 182 keV $K^\pi = \frac{9}{2}^-$, and 2462 keV $K^\pi = \frac{23}{2}^+$ have been observed in ^{129}Ba [10]. The half-lives of 16 ± 2 ns and 47 ± 2 ns [9,11], respectively, for the $\frac{9}{2}^-$ and $\frac{23}{2}^+$ isomeric states are favorable to observe the precession of the angular distribution pattern due to magnetic interaction differentially with respect to time (TDPAD technique). In the present investigation, the magnetic perturbation of the angular distribution pattern of the deexciting γrays from the respective isomeric states has been exploited for the calibration of the internal magnetic field at Ba in iron and for determination of the g factor of the isomeric states. An approximate value of the hyperfine magnetic field, -8.5 ± 1.4 T, at Ba in Fe [12] is known from earlier measurements, employing the perturbed angular distribution after ion implantation (IMPA) technique. One observes the integrated effect of different types of hyperfine interactions over the lifetime of the state through the IMPAD technique. Further, there is uncertainty in the lifetime of the state (mean lifetime in ps) used for the extraction of the magnitude of the magnetic hyperfine fields. In contrast, the different types of hyperfine interactions can be distinguished by the TDPAD technique, and the precessional frequencies are extracted directly without the knowledge of the lifetime of the state. The internal magnetic field in iron was calibrated with respect to the g factor, $-0.159(5)$, of the 10^+ isomeric state in ^{132}Ba [13] for precise g factor measurements.

II. EXPERIMENTAL DETAILS

The $\frac{9}{2}^-$ and $\frac{23}{2}^+$ isomeric states in ^{129}Ba (Fig. 1) were excited through the nuclear reaction ^{120}Sn(^{12}C, $3n\gamma$)^{129}Ba by a 52 MeV ^{12}C pulsed beam from the 15UD Pelletron accelerator facility at IUAC (New Delhi). The pulse repetition

*akbhati@pu.ac.in

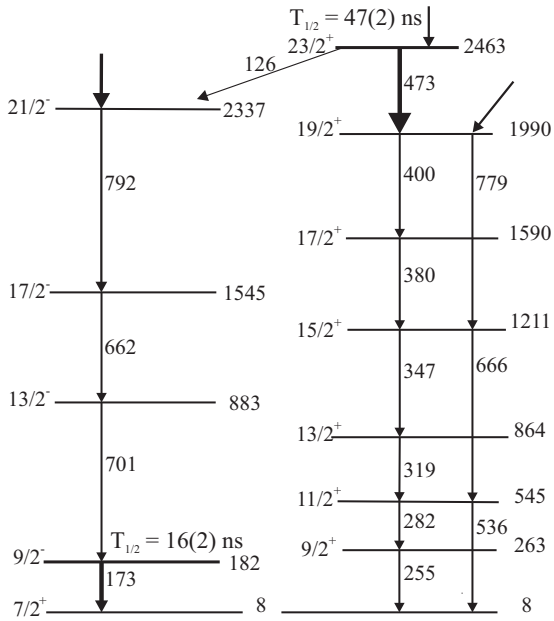

FIG. 1. Partial level decay scheme of $\frac{9}{2}^-$ and $\frac{23}{2}^+$ isomeric states in ^{129}Ba (weak transitions are omitted) [11]. The weakly populated $\frac{23}{2}^+$ state feeds the $\frac{9}{2}^-$[514] band indirectly through the 126 keV transition.

period was 250 ns. The target consisted of 500 μg/cm^2 ^{120}Sn evaporated on 1 mg/cm^2 iron foil backed by tantalum foil to stop the beam. The 99.99% pure iron foil after rolling to the desired thickness was annealed as described in Ref. [14], to get the saturated internal magnetic field at the recoil implanted Ba ions. The magnetizations of the foils were tested by magnetometer and showed good magnetic properties. In the second part of the experiment, the 10^+ isomeric state in ^{132}Ba was excited through the ^{124}Sn(^{12}C, $4n\gamma$)^{132}Ba reaction by a 62 MeV ^{12}C pulsed beam with 250 ns time interval to calibrate the internal magnetic field at Ba in Fe. The ^{120}Sn target was replaced by a ^{124}Sn target consisting of 700 μg/cm^2 ^{124}Sn evaporated on 1 mg/cm^2 annealed Fe foil. In these experiments the iron foil was polarized by a 0.2 T external magnetic field (measured by Hall probe) perpendicular to the detector plane. The external magnetic field was provided by a C-type electromagnet (homogeneity better than one in 10^4 in 2 cm^3 volume at 0.9 T field). The γ-rays from the respective isomeric states were detected by two high-purity germanium (HPGe) detectors of 25% efficiency and 2.1 keV energy resolution at 1332 keV γ rays. The detectors were positioned at $\pm 45^\circ$ with respect to the beam direction and placed at 25 cm distance from the target in the horizontal plane. The data were collected in the LIST mode with four parameters: the two energy and two time signals from time-to-pulse-height converters corresponding to each HPGe detector.

III. DATA ANALYSIS AND RESULTS

The acquired data, following proper gain matching for energy and time, were sorted offline into E_γ-t matrices corresponding to two detectors. These matrices were then used

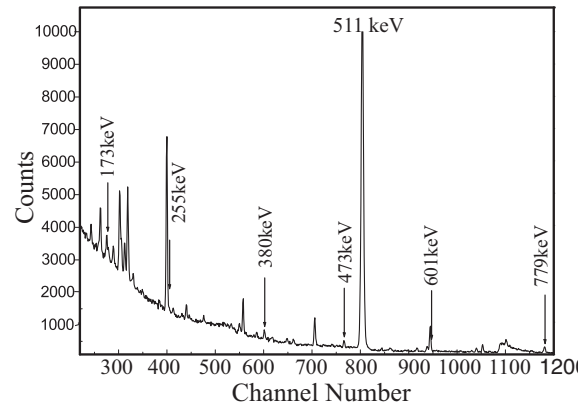

FIG. 2. Delayed γ-ray energy spectrum of ^{129}Ba without background subtraction.

to create time-gated energy spectra and energy-gated time spectra for the system. As an illustration, a typical delayed (20–200 ns gate) γ-ray energy spectrum in ^{129}Ba is projected in Fig. 2. The time spectra of both the HPGe detectors were added after matching the time zero ($T_\circ$), background subtraction and normalization. The summed time spectra were least-squares fitted to the exponential decay to extract the half-life times of the corresponding states. The resulting decay spectra for the $\frac{9}{2}^-$ and $\frac{23}{2}^+$ isomeric states in ^{129}Ba are shown in Fig. 3. The observed half-life times $T_{1/2}(\frac{9}{2}^-) = 15(1)$ ns and $T_{1/2}(\frac{23}{2}^+) = 47(1)$ ns are in good agreement with the results of previous measurements [9,11]. This shows the negligible indirect side feeding from the $\frac{23}{2}^+$ isomeric state to the $\frac{9}{2}^-$[514] band. The $\frac{23}{2}$ band is populated weakly compared to the $\frac{9}{2}^-$[514] band.

The $R(t)$ factors were formed from the background-subtracted and normalized time spectra $I(\theta, t)$,

$$R(t) = \frac{I(45^\circ, t) - I(-45^\circ, t)}{I(45^\circ, t) + I(-45^\circ, t)}. \quad (1)$$

The ratio factors $R(t)$ for the $\frac{9}{2}^-$, $\frac{23}{2}^+$ isomers in ^{129}Ba and 10^+ isomer in ^{132}Ba were least-squares fitted to the theoretical magnetic perturbation expression [15],

$$R_{\text{theor}} = \frac{3}{4} A_2 \exp(-\lambda t) \sin(2\omega_L t + \phi), \quad (2)$$

to extract the Larmor precession frequency ω_L ($= g\mu_N B/\hbar$). The angular distribution coefficients A_2, ω_L, phase angle ϕ for the bending of beam, and the damping constant $\lambda = (\frac{1}{\tau_{\text{rel}}})$ were kept as free parameters. The experimental ratio functions $R(t)$ and corresponding fits are depicted in Fig. 4.

The extracted magnetic hyperfine field with the value $-6.0(2)$ T at Ba in iron from the Larmor frequency of the 10^+ state [$g = -0.159(5)$] in ^{132}Ba is comparable with the earlier quoted value [12], but its measurement is more precise in the present work. The ratio of precession frequencies of the $\frac{9}{2}^-$ and $\frac{23}{2}^+$ states with respect to 10^+ state, i.e.,

$$\frac{\omega_L(\frac{9}{2}^-)}{\omega_L(10^+)} = 1.21 \pm 0.01 \quad \text{and} \quad \frac{\omega_L(\frac{23}{2}^+)}{\omega_L(10^+)} = 1.47 \pm 0.01, \quad (3)$$

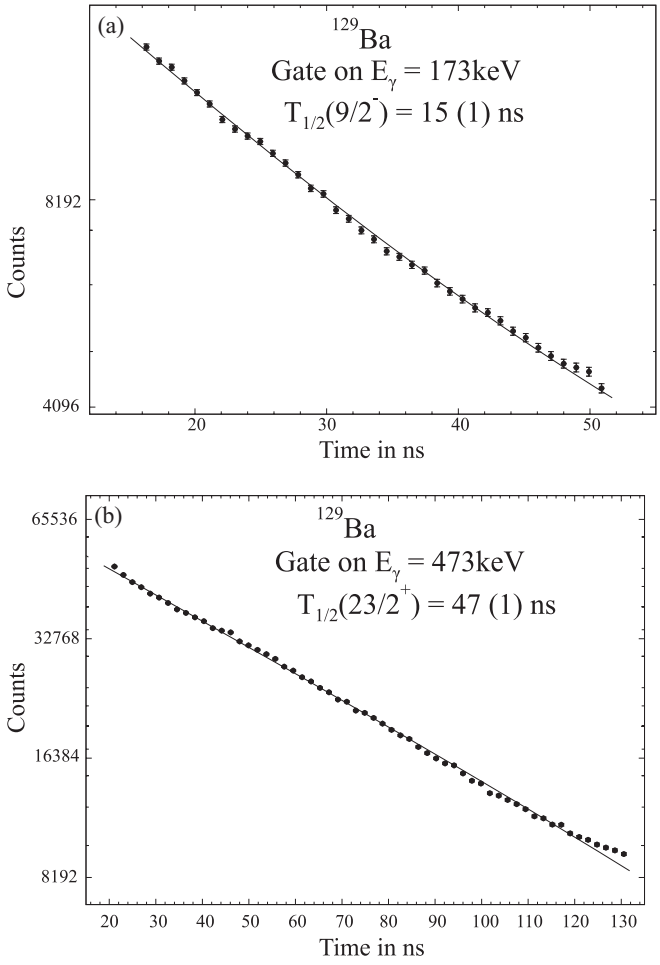

FIG. 3. Summed time spectra with gates on γ-ray transition from $\frac{9}{2}^-$ (a) and $\frac{23}{2}^+$ (b) isomeric states in ^{129}Ba. The solid curve shows the least-squares fit to the data.

is free from any uncertainty in the magnetic field value at Ba ions in iron. The value of g factors so deduced, $g(\frac{9}{2}^-) = -0.192(6)$ and $g(\frac{23}{2}^+) = -0.233(7)$, along with the corresponding values in the isotopic/isotonic chain of ^{129}Ba are tabulated in Table I. The sign of the g factor was determined from the direction of the rotation of the angular distribution pattern.

The data exhibit damping of the spin precession amplitude, which may be attributed to loss of alignment caused by the weak, randomly oriented quadrupole interaction due to radiation damage produced by recoiling ions in the Fe foil. We observed that the damping is not proportional to the magnetic moment of the states; rather it is related to the spectroscopic quadrupole moment (Q_s) of the respective states [16]. In a small time window of the TDPAD spectra, it is difficult to distinguish between static and dynamic nature of quadrupole interactions. We have approximated the effect of quadrupole interaction in the form of exponential damping with the damping constant proportional to the electric quadrupole interaction strength [16], i.e. $\lambda \propto (\omega_o \tau_c)^2$, to extract approximate values of Q_s for the respective isomeric states. The electric quadrupole frequency ω_o is defined for the half-integer spin I as $\frac{eQ_sV_{zz}}{4I(2I-1)\hbar}$.

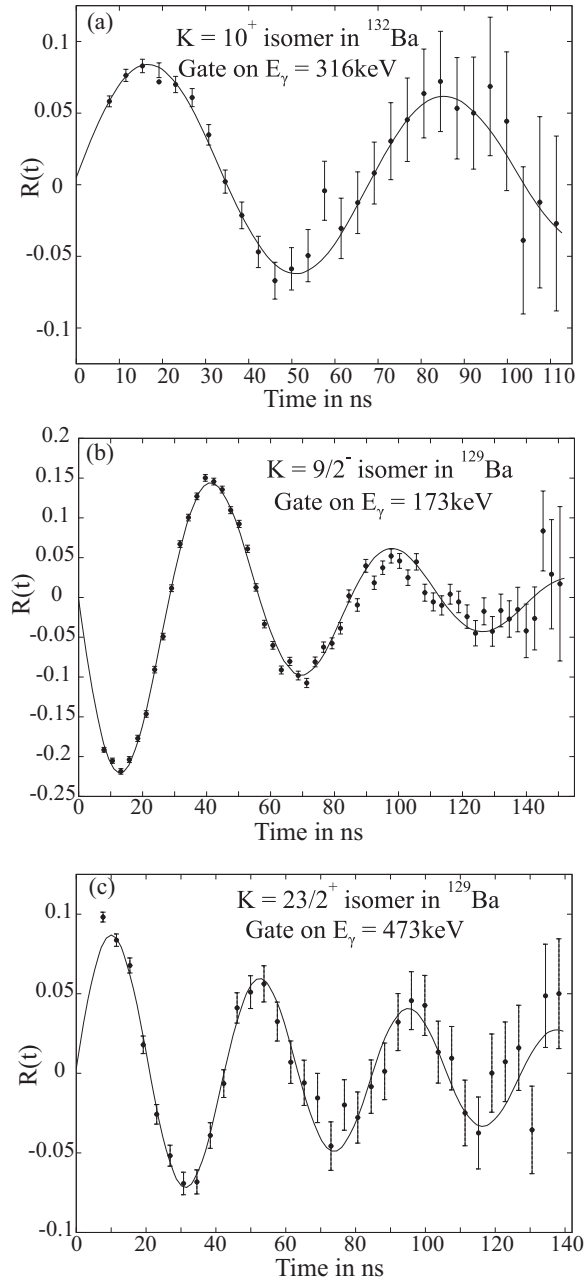

FIG. 4. Spin rotation spectra of the 10^+ (a) isomeric state in ^{132}Ba and the $\frac{9}{2}^-$ (b) and $\frac{23}{2}^+$ (c) isomeric states in ^{129}Ba implanted in the polarized iron at room temperature.

The average electric field gradient V_{zz} (static or fluctuating) depends on the correlation time τ_c, and it will be same for both the isomeric states. The value of the quadrupole moment ratio deduced from the ratio of relaxation time $\tau_{\rm rel}$ of the respective states, i.e., $\tau_{\rm rel}(\frac{9}{2}^-) = 70$ ns and $\tau_{\rm rel}(\frac{23}{2}^+) = 113$ ns, turns out to be $Q_s(\frac{9}{2}^-)/Q_s(\frac{23}{2}^+) = 1.3$.

IV. DISCUSSION

The $\frac{9}{2}^-$ level at 182 keV is a bandhead of the $K^\pi = \frac{9}{2}^-$ band exhibiting large signature splitting. The same type

TABLE I. Comparison of values of the g factors determined in the present work with the values in the isotopic/isotonic chain of ^{129}Ba [17] assuming $g_R = 0.35(3)$ [18].

Isomeric state	Nucleus	g factor	g_Ω
$\frac{5}{2}^+[402]$	^{123}Ba	−0.272(1)	−0.52(3)
$\frac{7}{2}^+[404]$	^{129}Ba	+0.266(1)	0.24(3)[a]
$\frac{7}{2}^-[523]$	^{127}Ba	−0.2065(2)	−0.36(3)
$\frac{9}{2}^-[514]$	^{125}Te	−0.20(1)	−0.32(3)
	^{127}Xe	−0.1965(3)	−0.31(3)
	^{129}Ba	−0.192(6)[b]	−0.31(3)
	^{131}Ba	−0.19(1)	−0.31(3)
	^{131}Ce	−0.19(1)	−0.31(3)
$\frac{11}{2}^-[505]$	^{133}Ba	−0.17(1)	−0.26(3)
$\frac{23}{2}^+$	^{129}Ba	−0.233(7)[b]	−0.28(3)

[a]Reference [19].
[b]Present work.

of band structure has been observed all over the Xe-Ba-Ce region. The state has been assigned a $\nu\frac{9}{2}^-[514]$ Nilsson configuration with parentage of the $h_{11/2}$ shell through in-beam γ-ray spectroscopic studies [9,11]. This is corroborated by the neutron pickup reaction ^{130}Ba$(d, t)^{129}$Ba studies [20,21] also. The observed g factor, −0.192(6), further confirms the $\nu h_{11/2}$ $\frac{9}{2}^-[514]$ configuration of the $\frac{9}{2}^-$ isomeric state. This is in nice agreement with the g factor values of $\frac{9}{2}^-$ isomeric states seen in $N = 73$ isotones and in the neighboring Ba nuclei, Table I. A good description of negative-parity bands is obtained within the RTRM formalism assuming $h_{11/2}$ neutron hole coupling to the rigid triaxial core (quadrupole deformation $\epsilon_2 \simeq 0.22$ and triaxiality parameter $\gamma \simeq 23^\circ$) [5]. The constancy of the g factor for the $\frac{9}{2}^-$ isomer in the $N = 73$ isotones or $Z = 56$ isotopes affirms the purity of the $\nu h_{11/2}$ configuration as per RTRM predictions [8].

The weakly populated band of the 2462 keV, $K^\pi = \frac{23}{2}^+$ state was observed by Byrne *et al.* [11]. They proposed a three-quasineutron configuration, $\frac{7}{2}^+[404] \otimes \frac{7}{2}^-[523] \otimes \frac{9}{2}^-[514]$, using the intraband and the interband analysis based on the semiclassical model of Dönau and Frauendorf [22]. However, they got poor agreement between the experimental and the calculated branching ratios, $\frac{B(M1)}{B(E2)}$, assuming the K value $\frac{23}{2}^+$ and $g_K - g_R = -0.43$. They attributed the discrepancy to the K mixing and suggested the effective K value $\frac{19}{2}$ or $\frac{21}{2}$. The g factor value, −0.056 was adopted considering the coupling of $h_{11/2}$ neutron hole with the 7^- isomeric state in ^{128}Ba. The measured g factor value, −0.233(7), by us is at variance with the results of the in-beam analysis. The sign of the g factor is in conformation with the three-quasineutron nature of the state but the value is somewhat larger than the adopted value. It is not surprising because, in the presence of γ deformation and the near degeneracy around the $\frac{23}{2}^+$ state (interaction strength between the bands based on $\frac{7}{2}^+$ and $\frac{23}{2}^+$ states is <2.5 keV), a pure three-quasineutron configuration cannot be expected. As indicated by the intraband analysis, the K mixing can give rise to the admixture of other three-quasineutron configurations. This is further evident from the observed quadrupole moment ratio = 1.3, which too is higher than the expected value 0.8 in the strong coupling approximation ($Q_s = \frac{3K^2 - I(I+1)}{(I+1)(2I+3)} Q_\circ$). The intrinsic quadrupole moment ($Q_\circ$) is expected to be same for both the $\frac{9}{2}^-$ and $\frac{23}{2}^+$ states, as both of these involve high-Ω orbitals in the $h_{11/2}$ shell. For the same intrinsic quadrupole moment the reduction of the K value (effective value of $K \approx \frac{19}{2}$) corresponds to the observed ratio 1.3, different from 0.8. Reduction of the K value due to K mixing was also observed in case of the 7^- isomer in ^{130}Ce [23], an isotone of ^{128}Ba, through the quadrupole moment measurements.

In the presence of triaxiality, the assignment of a unique value of K to the bandhead is unrealistic, as neither Ω nor K is a good quantum number. Different Ω subsystems may get mixed, and strong transitions connecting the subsystems may occur in the presence of triaxiality. Nonetheless, the nuclear moments are sensitive to the small mixing of different Ω wave functions. However, all the three particles participating in the excitation contribute to the quantity "effective K" and it seems quite difficult to disentangle them for configuration assignments. There is admixture of other three-quasineutron configurations involving high-Ω orbitals near the Fermi level [20], i.e., orbitals originating from the $g_{7/2}$ and $h_{11/2}$ shells. The configuration constrained potential-energy surface (PES) calculations [24] have predicted the excitation energies of two-quasineutron configurations, i.e., $\frac{7}{2}^+[404] \otimes \frac{7}{2}^-[523]$ and $\frac{5}{2}^+[402] \otimes \frac{7}{2}^-[523]$ within 300 keV. The coupling of a $h_{11/2}$ neutron hole with these configurations may give probable three-quasineutron configurations. In the absence of any theoretical calculation of the excitation energy of the three-quasiparticle energy states in Ba nuclei, we propose admixture of another configuration, $\nu\frac{5}{2}^+[402] \otimes \frac{7}{2}^-[523] \otimes \frac{11}{2}^-[505]$, in the adopted configuration. In a simplistic way the fraction of the admixtured configurations, i.e. (amp.)^2, can be evaluated based on the strong-coupling approximation. The g factor can be expressed as

$$g = g_R + (g_K - g_R)\frac{K^2}{I(I+1)} \quad \left(K \neq \frac{1}{2}\right) \tag{4}$$

for the bandhead; $K = I$, and g_K and g_R are the intrinsic and rotational g factors, respectively. The value of g_R is typically taken equal to $\frac{Z}{A}$ (hydrodynamical model) or the g factor of the ground band of the neighboring even-mass nuclei to estimate the value of g_K. Experimentally g_R is observed to have reduced value as compared to the hydrodynamical value because of pairing correlations. The value of g_K is relatively insensitive to g_R for large K. We have adopted $g_R = 0.35$ (3) from the g factor measurements of the ground band in $^{130-136}$Ba [18] isotopes, and the uncertainty in g_R is included in the extracted values of g_K. In case of multi-quasiparticle states, the intrinsic g_K factor can be estimated, based on Nilsson model, from the sum of intrinsic g factors g_{Ω_i}, using the following expression:

$$Kg_K = \sum_{i=1}^{3} \Omega_i g_{\Omega_i}, \quad K = \Omega_1 + \Omega_2 + \Omega_3. \tag{5}$$

The intrinsic g_{Ω_i} factors, extracted from the experimental magnetic moments of the low-lying states in the neighboring

odd-mass nuclei [17], are listed in Table I. The calculated g_K-factors for the $\nu\frac{7}{2}^+[404] \otimes \frac{7}{2}^-[523] \otimes \frac{9}{2}^-[514]$ and the $\nu\frac{5}{2}^+[402] \otimes \frac{7}{2}^-[523] \otimes \frac{11}{2}^-[505]$ configurations are -0.160 and -0.35, respectively. The measured value -0.286 lies in between and corresponds to about 0.34 admixture of $\frac{7}{2}^+[404] \otimes \frac{7}{2}^-[523] \otimes \frac{9}{2}^-[514]$ configuration to the main configuration $\frac{5}{2}^+[402] \otimes \frac{7}{2}^-[523] \otimes \frac{11}{2}^-[505]$ of the $\frac{23}{2}^+$ isomeric state. The multi-quasiparticle calculations (including residual nucleon-nucleon interaction and the triaxiality), similar to the $A \sim 180$ mass region, are desired to obtain the admixed configurations and their (amp.)^2, i.e., the fraction of the admixed configuration, precisely.

V. CONCLUSION

The precise g factor measurements of the $\frac{9}{2}^-$ and the $\frac{23}{2}^+$ isomeric states in ^{129}Ba have been carried out with reference to the 10^+ isomeric state in ^{132}Ba. The $g(\frac{9}{2}^-)$ factor has confirmed the pure one-quasiparticle neutron $\frac{9}{2}^-[514]$ nature of the $\frac{9}{2}^-$ bandhead of the unique parity bandhead. The $\frac{23}{2}^+$ isomeric state is proposed to have admixture of two configurations, $\nu\frac{5}{2}^+[402] \otimes \frac{7}{2}^-[523] \otimes \frac{11}{2}^-[505]$ and $\nu\frac{7}{2}^+[404] \otimes \frac{7}{2}^-[523] \otimes \frac{9}{2}^-[514]$, which is at variance with the pure three-quasineutron configuration $\frac{7}{2}^+[404] \otimes \frac{7}{2}^-[523] \otimes \frac{9}{2}^-[514]$, considered in the intraband analysis. Further, g factor and quadrupole moment measurements are in progress for the 7^- isomeric state in ^{128}Ba to get more information about the participating orbitals for the isomeric states.

ACKNOWLEDGMENTS

We are grateful to Hans-Jürgen Wollersheim (GSI) for providing the ^{124}Sn enriched target. We would like to thank accelerator crew, particularly S. Chopra, R. Joshi, and P. Barua for the stable pulsed beam and continuous support at the Inter-University Accelerator Centre during the experiment. One of us (J.K.) acknowledge financial assistance by the UGC/IUAC.

[1] A. Granderath, P. F. Mantica, R. Bengtsson, R. Wyss, P. von Brentano, A. Gelberg, and F. Seiffert, Nucl. Phys. A **597**, 427 (1996).
[2] R. Wyss, A. Granderath, R. Bengtsson, P. von Brentano, A. Dewald, A. Gelberg, A. Gizon, J. Gizon, S. Harissopulos, A. Johnson *et al.*, Nucl. Phys. A **505**, 337 (1989).
[3] P. M. Walker and K. Schiffer, Z. Phys. A **338**, 239 (1991).
[4] T. R. Saitol, N. Saitol-Hashimoto, G. Sletten, R. A. Bark, G. B. Hagemann, and B. Herskind, Phys. Scr. T **88**, 67 (2000).
[5] J. Yan, O. Vogel, P. von Brentano, and A. Gelberg, Phys. Rev. C **48**, 1046 (1993).
[6] A. Arima and F. Iachello, Ann. Phys. (N.Y.) **123**, 468 (1979).
[7] F. Iachello and P. van Isacker, *The Interacting Boson-Fermion Model* (Cambridge University Press, Cambridge, 1991).
[8] A. C. Mueller, F. Buchinger, W. Klempt, E. W. Otten, R. Neugart, C. Ekstrom, and J. Heinemeier, Nucl. Phys. A **403**, 234 (1983).
[9] J. Gizon, A. Gizon, and J. Meyer-Ter-Vehn, Nucl. Phys. A **277**, 464 (1977).
[10] Y. Tendov, Nucl. Data Sheets **77**, 631 (1996).
[11] A. P. Byrne, K. Schiffer, G. D. Dracoulis, B. Fabricius, T. Kibedi, A. E. Stuchbery, and K. P. Lieb, Nucl. Phys. A **548**, 131 (1992).
[12] H. W. Kugel, T. Polga, R. Kalish, and R. R. Borchers, Phys. Lett. B **32**, 463 (1977).
[13] P. Das, R. G. Pillay, V. V. Krishnamurthy, S. N. Mishra, and S. H. Devare, Phys. Rev. C **53**, 1009 (1996).
[14] P. Maier-Komor, K. H. Speidel, and A. Stolarz, Nucl. Instrum. Methods A **334**, 191 (1993).
[15] H. Frauenfelder and R. Steffen, in *Alpha- and Beta- and Gamma-Ray Spectroscopy*, edited by K. Siegbahn, Vol. 2 (North-Holland, Amsterdam, 1965), p. 997.
[16] A. Abragam and R. V. Pound, Phys. Rev. **92**, 943 (1953).
[17] N. J. Stone, At. Data Nucl. Data Tables **90**, 75 (2005).
[18] J. M. Brennan, M. Hass, N. K. B. Shu, and N. Benczer-Koller, Phys. Rev. C **21**, 574 (1980).
[19] K. Bekk, A. Andl, S. Goring, A. Hanser, G. Nowicki, H. Rebel, and G. Schatz, Z. Phys. A **291**, 219 (1979).
[20] R. D. Griffioen and R. K. Sheline, Phys. Rev. C **10**, 624 (1974).
[21] D. Bucurescu, J. Ott, W. Schauer, T. von Egidy, A. Gollwitzer, R. Hertenberger, A. Metz, G. Graw, B. D. Valnion, R. Meunier *et al.*, Nucl. Phys. A **630**, 643 (1998).
[22] F. Donau, Nucl. Phys. A **471**, 469 (1987).
[23] M. Ionescu-Bujor, A. Iordachescu, F. Brandolini, M. De Poli, N. H. Medina, P. Pavan, M. N. Rao, and C. Rossi Alvarez, Phys. Rev. C **60**, 024316 (1999).
[24] L. Hong-Liang and X. Fu-Rong, Chin. Phys. Lett. **25**, 1621 (2008).